Available online at www.sciencedirect.com
ScienceDirect
Journal of Power Sources 177 (2008) 493–499
JOURNAL OF POWER SOURCES
www.elsevier.com/locate/jpowsour

Thermodynamic analysis of the efficiency of high-temperature steam electrolysis system for hydrogen production

Liu Mingyi, Yu Bo*, Xu Jingming, Chen Jing

Institute of Nuclear and New Energy Technology, Tsinghua University, Beijing 100084, China

Received 1 October 2007; received in revised form 7 November 2007; accepted 7 November 2007
Available online 17 November 2007

Abstract

High-temperature steam electrolysis (HTSE), a reversible process of solid oxide fuel cell (SOFC) in principle, is a promising method for highly efficient large-scale hydrogen production. In our study, the overall efficiency of the HTSE system was calculated through electrochemical and thermodynamic analysis. A thermodynamic model in regards to the efficiency of the HTSE system was established and the quantitative effects of three key parameters, electrical efficiency (η_{el}), electrolysis efficiency (η_{es}), and thermal efficiency (η_{th}) on the overall efficiency ($\eta_{overall}$) of the HTSE system were investigated. Results showed that the contribution of η_{el}, η_{es}, η_{th} to the overall efficiency were about 70%, 22%, and 8%, respectively. As temperatures increased from 500 °C to 1000 °C, the effect of η_{el} on $\eta_{overall}$ decreased gradually and the η_{es} effect remained almost constant, while the η_{th} effect increased gradually. The overall efficiency of the high-temperature gas-cooled reactor (HTGR) coupled with the HTSE system under different conditions was also calculated. With the increase of electrical, electrolysis, and thermal efficiency, the overall efficiencies were anticipated to increase from 33% to a maximum of 59% at 1000 °C, which is over two times higher than that of the conventional alkaline water electrolysis.

Keywords: High-temperature steam electrolysis; Thermodynamic analysis; Overall efficiency; Hydrogen production; High-temperature gas-cooled reactor

1. Introduction

Large-scale hydrogen production without fossil fuel consumption and greenhouse gas emissions is the key to achieving the "hydrogen economy". Currently, massive hydrogen is produced primarily via steam methane reforming (SMR) and conventional alkaline water electrolysis. From a long-term perspective, methane reforming is not a viable process for massive hydrogen production, since such conversion processes consume fossil fuels and emit greenhouse gases [1–7]. Conventional alkaline water electrolysis is a well-established technique, which is capable of producing highly pure hydrogen without CO_2 emissions during the electrolysis process. However, this process consumes a lot of electricity which results in an unsatisfactory system efficiency (about 27%) and leads to high-operating costs [8]. An NREL report suggests that electricity costs comprise 80% of the total selling price of hydrogen from large-scale electrolysis [9].

The high-temperature steam electrolysis offers a promising method for highly efficient hydrogen production. Operation at high temperatures reduces the electrical energy requirement for the electrolysis and also increases the efficiency of the power-generating cycle. In addition, high-temperature systems can promote electrode activity and lessen the overpotential. Therefore, it is possible to increase the electric current density and consequently decrease the polarization losses at high temperatures, which improves the hydrogen production density and the electrolysis efficiency. Thus, the HTSE process is advantageous from both thermodynamic and kinetic standpoints [10,11].

The HTGR coupled with the HTSE system can ensure high-temperature steam electrolysis due to the high-outlet temperature of HTGR (up to 950 °C), thus, the process is expected to achieve very high and satisfactory thermal conversion

Abbreviations: HTSE, high-temperature steam electrolysis; HTGR, high-temperature gas-cooled reactor; SMR, steam methane reforming; HTR-10, high-temperature reactor-10; HHV, high-heating value of hydrogen; SOEC, solid oxide electrolysis cell; SOFC, solid oxide fuel cell; SI, sulfur-iodine.

* Corresponding author. Tel.: +86 10 80194039; fax: +86 10 62771740.
E-mail addresses: liumy06@mails.tsinghua.edu.cn (L. Mingyi), cassy_yu@mail.tsinghua.edu.cn (Y. Bo), xujingming@tsinghua.edu.cn (X. Jingming), jingxia@tsinghua.edu.cn (C. Jing).

0378-7753/$ – see front matter © 2007 Elsevier B.V. All rights reserved.
doi:10.1016/j.jpowsour.2007.11.019

Nomenclature

ΔC_p	heat capacity change of the reaction (J mol^{-1} K^{-1})
E	Nernst potential (V)
F	Faraday constant (C mol^{-1})
ΔG	Gibbs free energy change of the reaction (kJ mol^{-1})
ΔH	enthalpy change of the reaction (kJ mol^{-1})
i	operating current density (A cm^{-2})
n	number of electrons transferred ($n=2$)
Q	heat (kJ)
Q_{el}	consumed thermal energy used for generating electricity
$Q_{H,out}$	thermal energy of unit amount of the produced hydrogen
$Q_{overall}$	total thermal energy demand in the electrolysis process
Q_{th}	consumed thermal energy in the electrolysis process
ΔS	entropy change of the reaction (kJ mol^{-1} K^{-1})
T	temperature (K)
V_{th}	thermoneutral potential (V)
V_{op}	operating voltage (V)

Greek symbols

η_{el}	electrical efficiency of HTSE system
$\eta_{electrochem}$	electrochemical efficiency of SOEC system
η_{es}	electrolysis efficiency of HTSE system
$\eta_{faraday}$	Faradaic efficiency of SOEC system
$\eta_{overall}$	overall efficiency of HTSE system
η_{system}	system efficiency of SOEC system
η_{th}	thermal efficiency of HTSE system

efficiency while avoiding the challenging chemistry and corrosion issues associated with the thermochemical processes. A 10-MW high-temperature gas-cooled test reactor, the High-Temperature Reactor-10 (HTR-10), was operated in 2000 at the Institute of Nuclear and New Energy Technology (INET), Tsinghua University, Beijing. This test reactor can be utilized to develop a modular high-temperature gas-cooled reactor technology, as well as to establish an experimental base for nuclear process heat application. INET has started R&D projects for nuclear hydrogen production through an iodine-sulfur (IS) process and a HTSE process which are currently being considered as potential heat utilization systems for HTR-10. But until now, few studies have been conducted on the practical limits for the $\eta_{overall}$ of the HTSE system. Therefore, the objective of this paper is to examine, in detail, the theoretical efficiency of the HTSE system and determine the quantitative and qualitative effects of various factors on the overall efficiency of the HTSE system.

2. The HTSE system

Fig. 1 shows the schematic of the HTSE system. It consists of two parts, the primary energy system and the solid oxide

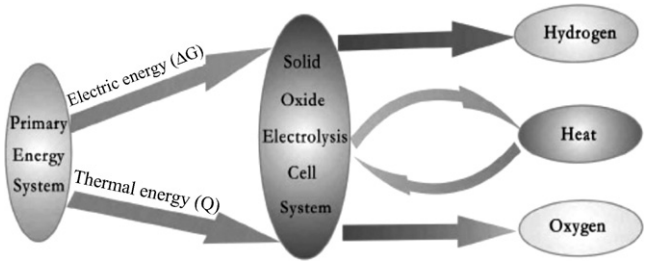

Fig. 1. Schematic of the HTSE system.

electrolysis cell (SOEC) system. HTGR is used as primary energy for the HTSE system and provides electrical energy as well as thermal energy to the SOEC system, where the high-temperature steam is electrolyzed to produce hydrogen and oxygen. The SOEC reported by Doenitz and Erdle was made of yttria-stabilized zirconia (YSZ) electrolyte, nickel–zirconia cermet (Ni + YSZ) cathode and strontium-doped lanthanum manganite (LSM) anode [4]. The electrolysis efficiency under the operating temperature of 997 °C was estimated at about 94% [13]. Another SOEC (Hino et al.) was made of yttria-stabilized zirconia (YSZ) electrolyte, nickel–zirconia cermet (Ni + YSZ) cathode and $LaCoO_3$ anode. The maximum electrolysis efficiency at the operating temperature of 950 °C was 86% at a current density of 98 mA cm^{-2} [13].The waste heat can be reused in the HTSE system, thus, improving the thermal efficiency.

In addition to operating temperature, the electrical efficiency (η_{el}), electrolysis efficiency (η_{es}), and thermal efficiency (η_{th}) have significant influence on the overall efficiency ($\eta_{overall}$) of the HTSE system. The η_{el} refers to the power-generation efficiency of HTGR and is given by

$$\eta_{el} = \frac{\Delta G}{Q} \tag{1}$$

where ΔG is the generated electrical energy and Q is the consumed thermal energy used for generating electricity.

The η_{es} refers to the overall efficiency of the SOEC system, including electrochemical efficiency ($\eta_{electrochem}$), Faradaic efficiency ($\eta_{Faraday}$), and system efficiency (η_{system}). $\eta_{electrochem}$ is $V_{op}(i,T)/E(T)$, in which $V_{op}(i,T)$ is approximately proportional to current density i at elevated temperature, where $V_{op}(i,T)$ is the operating voltage of the SOEC system at a given current density i and operating temperature T, and $E(T)$ is Nernst potential of the SOEC system at temperature T. η_{system} is the parasitic energy consumption of the SOEC system resulting from parasitic losses, such as resistance of pipeline, pumping work, ac–dc conversion, etc. The η_{es} is given by

$$\eta_{es} = \eta_{eletrochem}\eta_{Faraday}\eta_{system} \tag{2}$$

The η_{th} refers to the thermal utilization efficiency of the HTSE system. It considers the thermal exchange efficiency between the HTGR and the SOEC system, the heat dissipation of the HTSE system, the heat consumption for preheating excess steam, hydrogen at the cathode, and oxygen at the anode, as well

as the waste heat recycling. The η_{th} is given by

$$\eta_{th} = \frac{Q_{SOEC}}{Q_{HTGR}} = \frac{T_{inlet} - T_{outlet}}{T_{inlet}} \quad (3)$$

where Q_{HTGR} is the thermal energy from HTGR, Q_{SOEC} is the consumed thermal energy in the SOEC system, T_{inlet} is the outlet temperature of HTGR, and T_{outlet} is the outlet temperature of the SOEC system.

3. Thermodynamic model

3.1. Thermodynamics of steam electrolysis

The reaction of steam electrolysis is given by

$$H_2O \rightarrow H_2 + (1/2)\,O_2 \quad (4)$$

The total energy required $\Delta H(T)$ is $Q(T)$ and $\Delta G(T)$

$$\Delta H(T) = \Delta G(T) + Q(T) \quad (5)$$

where $Q(T) = T\Delta S(T)$.The thermoneutral potential $V_{tn}(T)$ is given by $V_{tn}(T) = \Delta H(T)/2F$, where $\Delta H(T)$ is the standard enthalpy of the reaction at T.

Standard thermodynamic parameters such as $\Delta H(T)$, $\Delta G(T)$, and $\Delta S(T)$ are functions of temperature. Therefore, the standard thermodynamic parameters at different temperatures can be calculated according to Kirchhoff's equation, entropy equation and the relation between ΔG and Nernst potential. These equations are given by [12]:

$$\Delta H(T) = \Delta H^{\circ}{}_{298.15} + \int_{298.15}^{T} \Delta C_p\,dT \quad (6)$$

$$\Delta S(T) = S^{\circ}{}_{298.15} + \int_{298.15}^{T} \frac{\Delta C_p}{T}\,dT \quad (7)$$

$$E(T) = -\frac{\Delta G(T)}{nF} \quad (8)$$

The Nernst potential at temperature T from Eq. (8) is considered to be under the standard pressure conditions for reactants and products. Table 1 shows the standard thermodynamic parameters at 298.15 K and 101.325 kPa. The thermodynamic parameters at the range of 298.15–1473.15 K were calculated according to Eqs. (6)–(8) and shown in Fig. 2. The results show that $\Delta H(T)$ increases slightly with the increase of temperatures, while $\Delta G(T)$ decreases, due to the increase of $Q(T)$. The ratio of $\Delta G(T)$ to $\Delta H(T)$ is about 93% at 373.15 K and about 70% at 1273.15 K. The decrease demand of electrical energy increases the thermal-to-hydrogen energy conversion efficiency. In addition, the high temperature also promotes electrode activity and lessens the cathodic and anodic overpotential, which decreases the energy loss and increases the η_{es} during the steam electrolysis process. Therefore, higher $\eta_{overall}$ for hydrogen production can be expected at higher operating temperatures [10,13].

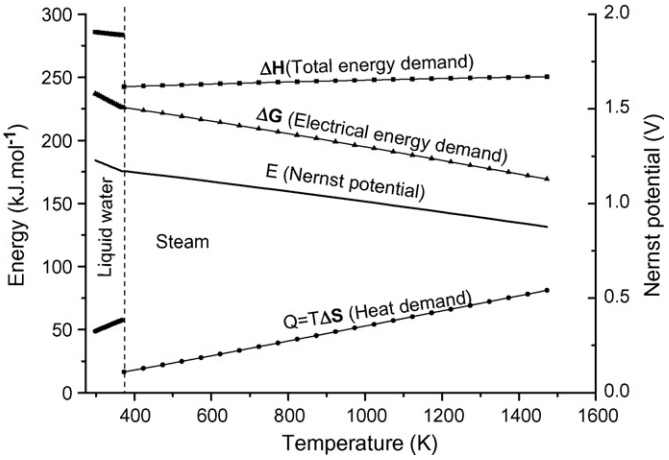

Fig. 2. Energy demand for water and steam electrolysis.

3.2. Efficiency modeling of the HTSE system

The electrical energy consumed in the electrolysis process can be expressed as

$$\Delta G = \eta_{el} Q_{el} \quad (9)$$

where Q_{el} is the consumed thermal energy from HTGR used for generating electricity. Then, the total thermal energy ($Q_{overall}$) required in the electrolysis process from HTGR can be expressed as

$$Q_{overall} = Q_{el} + Q_{th} = 2F\left[\frac{V_{op}(i,T)}{\eta_{el}} + \frac{V_{th}(T) - V_{op}(i,T)}{\eta_{th}}\right] \quad (10)$$

where Q_{el} and $2FV_{op}(i,T)/\eta_{el}$ is the consumed thermal energy for generating electricity, and Q_{th} and $2F(V_{th}(T) - V_{op}(i,T))/\eta_{th}$ is the thermal energy demand in the electrolysis process.

The $\eta_{overall}$ of the HTSE system can be defined as the ratio of the energy carried by unit amount of produced hydrogen ($Q_{H,out}$), in terms of a high-heat value of hydrogen (HHV = 285.8 kJ mol^{-1}), to the $Q_{overall}$ in the steam electrolysis process [10]. Therefore, the $\eta_{overall}$ can be expressed as

$$\eta_{overall} = \frac{Q_{H,out}}{Q_{overall}} = \frac{HHV}{Q_{el} + Q_{th}} = \frac{HHV}{[2F(V_{op}(i,T)/\eta_{el} + (V_{th}(T) - V_{op}(i,T)/\eta_{th})]} \quad (11)$$

Following Eqs. (5) and (8), and the equation of $E(T)/V_{op}(i,T) = \eta_{es}$, Eq. (11) then becomes:

$$\eta_{overall} = \frac{HHV}{\Delta G(T)/\eta_{el}\eta_{es} + Q_{th}(T)/\eta_{th} - (\Delta G(T)/\eta_{el}\eta_{th})(1 - \eta_{th})} \quad (12)$$

where $\Delta G(T)/\eta_{el}\eta_{es}$ is the actual thermal energy consumed for electricity generation.

$Q_{th}(T)/\eta_{th} - (\Delta G(T)/\eta_{el}\eta_{th})(1 - \eta_{es})$ is the actual thermal energy demand in the electrolysis process, where

Table 1
[12,14] Thermodynamic parameters for the HTSE at 298.15 K and 101.325 kPa

	ΔG (kJ mol^{-1})	ΔH(kJ mol^{-1})	S (kJ mol^{-1})	$\Delta V_{ap}H$ (kJ mol^{-1})	Heat capacity (C_p J mol^{-1} K^{-1})
H_2 (g)	0	0	0.131	–	$(29.07–0.836) \times 10^{-3}T + 20.1 \times 10^{-7}T^2$
O_2 (g)	0	0	0.205	–	$(25.72 + 12.98) \times 10^{-3}T - 38.6 \times 10^{-7}T^2$
H_2O (l)	237.2	285.8	0.07	40.7	75.30
H_2O (g)	–	–	–	–	$(30.36 + 9.61) \times 10^{-3}T + 11.8 \times 10^{-7}T^2$

(g) and (l) refer to gas phase and liquid phase, respectively.

$(\Delta G(T)/\eta_{el}\eta_{th})(1-\eta_{es})$ is the thermal energy converted from polarization and Ohmic losses during the electrolysis process.

We can see that $\eta_{overall}$ is examined as a function of individual efficiencies of η_{el}, η_{es}, and η_{th}, which cover almost all of the energy losses in the actual HTSE process for hydrogen production.

The total differential equation of the $\eta_{overall}$ is written as

$$d\eta_{overall} = \frac{\partial\eta_{overall}}{\partial\eta_{el}} d\eta_{el} + \frac{\partial\eta_{overall}}{\partial\eta_{es}} d\eta_{es} + \frac{\partial\eta_{overall}}{\partial\eta_{th}} d\eta_{th} \quad (13)$$

where

$$\frac{\partial\eta_{overall}}{\partial\eta_{el}} = \frac{HHV \times \Delta G(T)/\eta_{es}}{[\Delta G(T)/\eta_{el}\eta_{es} + Q_{th}(T)/\eta_{th} - (\Delta G(T)/\eta_{es}\eta_{th})(1-\eta_{es})]^2\eta_{el}^2} \quad (14)$$

$$\frac{\partial\eta_{overall}}{\partial\eta_{es}} = \frac{HHV \times \Delta G(T)(1/\eta_{el} - 1/\eta_{th})}{[\Delta G(T)/\eta_{el}\eta_{es} + Q_{th}(T)/\eta_{th} - (\Delta G(T)/\eta_{es}\eta_{th})(1-\eta_{es})]^2\eta_{es}^2} \quad (15)$$

$$\frac{\partial\eta_{overall}}{\partial\eta_{th}} = \frac{HHV \times [Q_{th} - (\Delta G(T)/\eta_{es})(1-\eta_{es})]}{[\Delta G(T)/\eta_{el}\eta_{es} + Q_{th}(T)/\eta_{th} - (\Delta G(T)/\eta_{es}\eta_{th})(1-\eta_{es})]^2\eta_{th}^2} \quad (16)$$

In order to analyze the effects of η_{el}, η_{es}, and η_{th} on $\eta_{overall}$, the range of each variable parameter was assumed as follows:

(1) η_{el}: 40–52%
(2) η_{es}: 60–100%
(3) η_{th}: 30–90%
(4) T: 500–1000 °C.

4. Results and discussion

4.1. Effect of η_{el}

Fig. 3 shows the effect of η_{el} on $\eta_{overall}$. As shown in Fig. 3, the η_{el} has a significant effect on the $\eta_{overall}$, for $\partial\eta_{overall}/\partial\eta_{el}$ values in the range of 1.175 and 1.062, which reveals that $\eta_{overall}$ changes more than one unit when the η_{el} changes one unit. On the other hand, as η_{el} increased from 40% to 52%, the effect of η_{el} on $\eta_{overall}$ decreased gradually with a linear relationship at different temperatures. And with the increase of T from 500 °C to 1000 °C, the effect of η_{el} on $\eta_{overall}$ also decreased gradually and the reducing velocities of the $\partial\eta_{overall}/\partial\eta_{el}$ values raised with the increase of η_{el}. Therefore, the effect of η_{el} on $\eta_{overall}$ decreased with increasing η_{el} and T.

4.2. Effect of η_{es}

As shown in Fig. 4, the effect of η_{es} on $\eta_{overall}$ is not as observable as η_{el}. The values of $\partial\eta_{overall}/\partial\eta_{es}$ are only in the range of

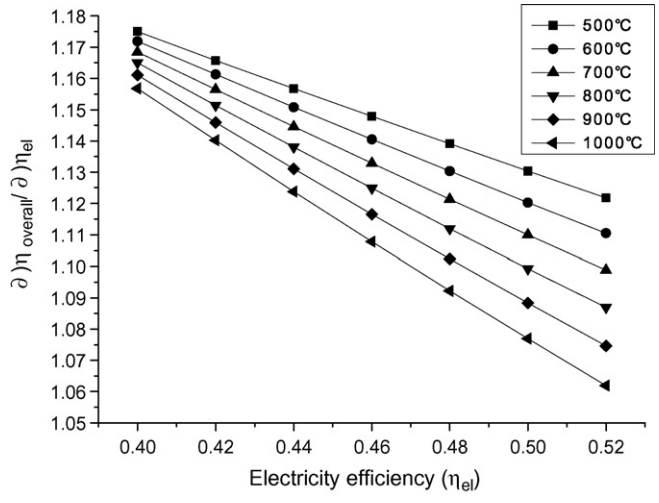

Fig. 3. Effect of η_{el} on $\eta_{overall}$ (η_{es}: 100%, η_{th}: 90%).

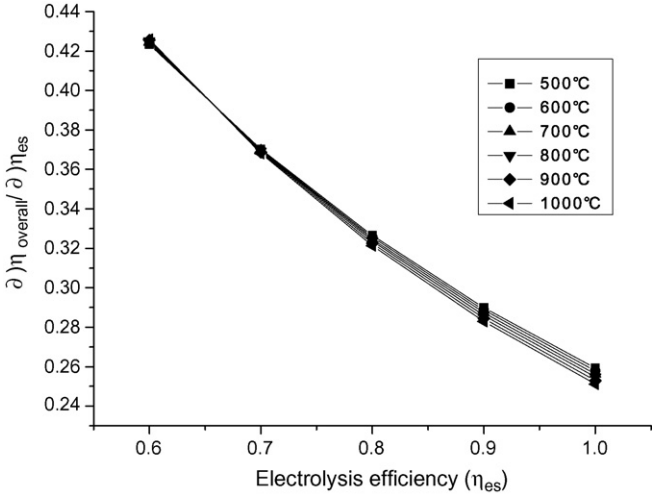

Fig. 4. Effect of η_{es} on $\eta_{overall}$ (η_{el}: 45%, η_{th}: 90%).

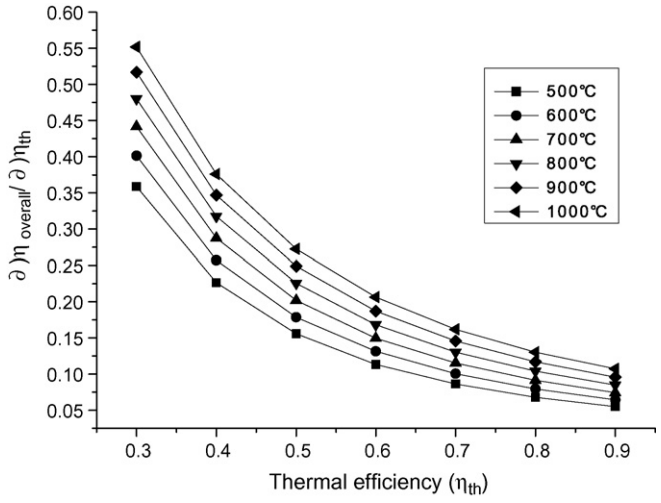

Fig. 5. Effect of η_{th} on $\eta_{overall}$ (η_{el}: 45%, η_{es}: 100%).

Table 2
The $\partial\eta_{overall}/\partial\eta_{el}$ values of different η_{el} at various temperatures

Temperature (°C)	η_{el}						
	0.4	0.42	0.44	0.46	0.48	0.50	0.52
500	1.175	1.1658	1.1568	1.1479	1.1391	1.1304	1.1218
600	1.1719	1.1613	1.1508	1.1405	1.1304	1.1203	1.1105
700	1.1685	1.1565	1.1446	1.1329	1.1214	1.11	1.0988
800	1.165	1.1514	1.138	1.1249	1.112	1.0993	1.0869
900	1.1611	1.1459	1.1311	1.1166	1.1023	1.0883	1.0746
1000	1.1568	1.1402	1.1238	1.1078	1.0922	1.0769	1.0619

0.426 and 0.251. With the increase of η_{es} from 60% to 100%, the effect of η_{es} on $\eta_{overall}$ decreased at different temperatures, and the trends were non-linear. On the other hand, as temperatures increased from 500 °C to 1000 °C, the effect of η_{es} on $\eta_{overall}$ almost stayed constant, as shown in Fig. 4, which demonstrated that the operating temperatures had little influence on the effect of η_{es} on $\eta_{overall}$.

4.3. Effect of η_{th}

Fig. 5 shows the effect of η_{th} on $\eta_{overall}$. With the increase of η_{th} from 30% to 90%, the effect of η_{th} on $\eta_{overall}$ diminished rapidly at different temperatures, as shown in Fig. 5. The changing trends showed the exponential relationship, which revealed that the values of $\partial\eta_{overall}/\partial\eta_{th}$ changed rapidly at low η_{th} (e.g.

Table 3
The $\partial\eta_{overall}/\partial\eta_{es}$ values of different η_{es} at various temperatures

Temperature (°C)	η_{es}				
	0.6	0.7	0.8	0.9	1
500	0.4234	0.3702	0.3264	0.2899	0.2593
600	0.4239	0.3699	0.3255	0.2887	0.2578
700	0.4245	0.3695	0.3246	0.2874	0.2562
800	0.4250	0.3691	0.3236	0.2860	0.2546
900	0.4255	0.3687	0.3225	0.2845	0.2529
1000	0.4259	0.3681	0.3213	0.2830	0.2511

Table 4
The $\partial\eta_{overall}/\partial\eta_{th}$ values of different η_{th} at various temperatures

Temperature (°C)	η_{th}				
	0.5	0.6	0.7	0.8	0.9
500	0.1556	0.1136	0.0865	0.0681	0.055
600	0.1787	0.1314	0.1007	0.0796	0.0645
700	0.202	0.1496	0.1153	0.0915	0.0744
800	0.2254	0.1682	0.1304	0.104	0.0848
900	0.2489	0.1872	0.1459	0.1169	0.0958
1000	0.2725	0.2066	0.162	0.1304	0.1072

Table 5
The average values of $\partial\eta_{overall}/\partial\eta_{efficiency}$ at various temperatures

Temperature (°C)	Normalized average values of $\partial\eta_{overall}/\partial\eta_{efficiency}$		
	$\partial\eta_{overall}/\partial\eta_{el}$	$\partial\eta_{overall}/\partial\eta_{es}$	$\partial\eta_{overall}/\partial\eta_{th}$
500	72.771	21.160	6.070
600	71.978	21.020	7.002
700	71.173	20.879	7.948
800	70.353	20.734	8.912
900	69.521	20.588	9.891
1000	68.676	20.437	10.888

below 50%), and changed slowly with the increase of η_{th}. The values of $\partial\eta_{overall}/\partial\eta_{th}$ dramatically decreased from 0.552 to 0.055 when η_{th} escalated from 30% to 90%. During practical operating processes, the η_{th} of the HTSE system is usually above 50%. Therefore, η_{th} values from 50% to 90%, which corresponds to $\partial\eta_{overall}/\partial\eta_{th}$ values between 0.272 and 0.055, do not have as much effect on $\eta_{overall}$ as compared to η_{el} and η_{es}. Consequently, the qualitative effects of electrical, electrolysis, and thermal efficiency on $\eta_{overall}$ can be ordered as $\eta_{el} > \eta_{es} > \eta_{th}$, which is consistent with the conclusion by Shin et al. [8]. The quantitative effects on the $\eta_{overall}$ are shown in the next section.

In addition, as temperatures increased from 500 °C to 1000 °C, the effect of η_{th} on $\eta_{overall}$ increased gradually, as

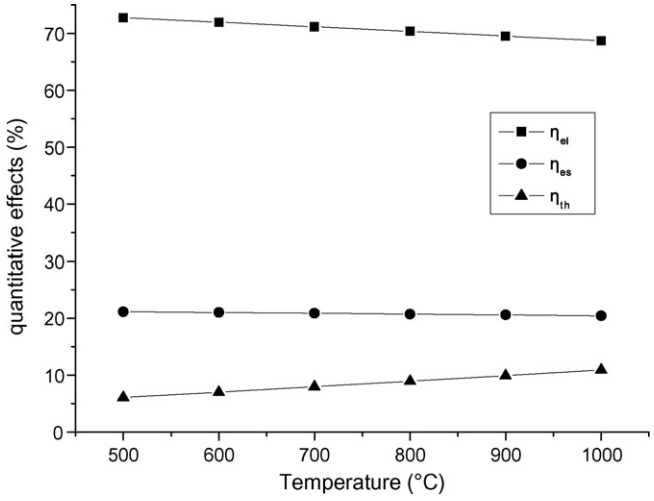

Fig. 6. Quantitative effects of η_{el}, η_{es}, and η_{th} on $\eta_{overall}$ at various temperatures.

Table 6
Electrical efficiencies of HTGR at different temperatures

Temperature (°C)	η_{el} (%)
500	40
600	42
700	45
800	47
900	50
1000	52

shown in Fig. 5. This is in contrast to what was seen for η_{el} (Fig. 3). This demonstrated that the effect of η_{th} on $\eta_{overall}$ diminished with increasing η_{th} and decreasing operating temperatures.

4.4. Quantitative analysis of the η_{el}, η_{es}, and η_{th} effects

Tables 2–4 shows the $\partial\eta_{overall}/\partial\eta_{efficiency}$ values of different efficiencies at various temperatures. As shown in these tables, the values of $\partial\eta_{overall}/\partial\eta_{efficiency}$ are variable at different efficiencies and temperatures, but the distinction of these values are not significant. Therefore, the average values of $\partial\eta_{overall}/\partial\eta_{efficiency}$ at different efficiencies are calculated and normalized, shown in Table 5, for quantitative comparison of the effects of η_{el}, η_{es}, and η_{th} on $\eta_{overall}$ at different temperatures. Fig. 6 obtained from Table 5 illustrates the quantitative effects of η_{el}, η_{es}, and η_{th}. With the increase of temperatures, the η_{el} effects decrease slightly, and the η_{th} effects increase slightly, while the η_{es} effects stay almost constant which are similar to the conclusions reached in Sections 4.1–4.3. The quantitative effects of the η_{el}, η_{th}, and η_{th} are about 70%, 22%, and 8%, respectively.

Table 7
Overall system efficiencies under various conditions

η_{es}	$\eta_{overall}$				
	$\eta_{th}=50\%$	$\eta_{th}=60\%$	$\eta_{th}=70\%$	$\eta_{th}=80\%$	$\eta_{th}=90\%$
$T=500\,^{\circ}C$ ($\eta_{el}=40\%$)					
60%	0.3704	0.3530	0.3415	0.3334	0.3273
80%	0.3961	0.3935	0.3917	0.3903	0.3892
100%	0.4132	0.4226	0.4295	0.4348	0.4391
$T=600\,^{\circ}C$ ($\eta_{el}=42\%$)					
60%	0.3971	0.3790	0.3671	0.3586	0.3523
80%	0.4186	0.4174	0.4166	0.4160	0.4155
100%	0.4327	0.4445	0.4533	0.4602	0.4656
$T=700\,^{\circ}C$ ($\eta_{el}=45\%$)					
60%	0.4360	0.4165	0.4037	0.3945	0.3877
80%	0.4504	0.4510	0.4515	0.4518	0.4520
100%	0.4595	0.4746	0.4860	0.4949	0.5020
$T=800\,^{\circ}C$ ($\eta_{el}=48\%$)					
60%	0.4746	0.4544	0.4409	0.4313	0.4242
80%	0.4807	0.4837	0.4859	0.4875	0.4888
100%	0.4845	0.5032	0.5175	0.5288	0.5379
$T=900\,^{\circ}C$ ($\eta_{el}=50\%$)					
60%	0.5000	0.4805	0.4675	0.4582	0.4513
80%	0.5000	0.5057	0.5099	0.5130	0.5155
100%	0.5000	0.5221	0.5392	0.5527	0.5637
$T=1000\,^{\circ}C$ ($\eta_{el}=52\%$)					
60%	0.5243	0.5062	0.4941	0.4854	0.4788
80%	0.5180	0.5268	0.5333	0.5383	0.5422
100%	0.5143	0.5400	0.5600	0.5760	0.5890

4.5. Calculations of the $\eta_{overall}$

According to the research progress on the HTR-10 in Tsinghua University, the actual electrical efficiencies of HTGR at different temperatures, shown in Table 6, were assumed [15]. Table 7 shows the calculated results of the overall system efficiencies under various conditions. As shown in Table 7, with the increase of η_{el}, η_{es}, and η_{th}, the overall system efficiencies are anticipated to be from 33% to 59%, and the maximum $\eta_{overall}$ can reach 59% at 1000 °C. Compared with the $\eta_{overall}$ of well developed conventional alkaline water electrolysis, which is about 27%, the efficiency of the HTGR coupled with the HTSE system is over two times higher than that of the conventional alkaline water electrolysis.

With the increase of temperatures, not only does the electrical energy demand reduce greatly, but η_{el} and η_{es}, which influence much on the $\eta_{overall}$, are also improved significantly. As a result, the $\eta_{overall}$ of the HTSE system is highly increased. Therefore, the HTSE system is much more efficient than low-temperature water electrolysis systems such as alkaline water electrolysis and solid polymer electrolyte (SPE) water electrolysis. This HTSE system can be considered as a promising way for highly efficient large-scale hydrogen production.

5. Conclusions

In this work, the overall efficiency of the HTSE system was analyzed. A thermodynamic model of the HTSE system efficiency was established, and the effects of η_{el}, η_{es}, and η_{th} on $\eta_{overall}$ of the HTSE system were investigated. Furthermore, the overall efficiencies of the HTSE system under different conditions were calculated. The results showed that:

The qualitative effects of electrical, electrolysis and thermal efficiency on the $\eta_{overall}$ were in the order $\eta_{el} > \eta_{es} > \eta_{th}$. The quantitative effects of η_{el}, η_{th}, and η_{th} were about 70%, 22%, and 8%, respectively.

As temperatures increased from 500 °C to 1000 °C, the effect of η_{el} on $\eta_{overall}$ decreased gradually, and the effect of η_{es} stayed almost constant, while the effect of η_{th} increased gradually.

The $\eta_{overall}$ of the HTGR coupled with the HTSE system were expected to increase from 33% to a maximum of 59% at 1000 °C, which is over two times higher than that of the conventional alkaline water electrolysis.

Acknowledgements

This work was supported by the 985 key project "HTSE technology for Hydrogen Production Research" of Tsinghua University. The authors would like to thank Wang Dengying, Bai Ying, and Gao Jie for their help and assistance.

References

[1] A. Hauch, S.H. Jensen, S. Ramousse, M. Mogensen, J. Electrochem. Soc. 153 (2006) A1741–A1747.

[2] J. Stephen Herring, J.E. O'Brien, C.M. Stoots, G.L. Hawkes, J.J. Gartvigsen, Mehrdad Shahnam, Int. J. Hydrogen Energy 32 (2007) 440–450.

[3] J. Udagawa, P. Aguiar, N.P. Brandon, J. Power Sources 166 (2007) 127–136.

[4] W. Doenitz, E. Erdle, Int. J. Hydrogen Energy 10 (1985) 291–295.

[5] H.S. Hong, U.-S. Chae, S.-T. Choo, K.S. Lee, J. Power Sources 149 (2005) 84–89.

[6] Nuclear Hydrogen Initiative—Ten Year Program Plan, DOE Office, USA, March 2005, pp. 31–34.

[7] J.E. O'Brien, C.M. Stoots, J.S. Herring, J. Hartvigsen, J. Fuel Cell Sci. Technol. 3 (2006) 213–219.

[8] Y. Shin, W. Park, J. Chang, J. Park, Int. J. Hydrogen Energy 32 (2007) 1486–1491.

[9] A. Roy, S. Watson, D. Infield, Int. J. Hydrogen Energy 31 (2006) 1964–1979.

[10] B. Yildiz, M.S. Kazimi, Int. J. Hydrogen Energy 31 (2006) 77–92.

[11] K. Eguchi, T. Hatagishi, H. Arai, Solid State Ionics 86–88 (1996) 1245–1249.

[12] F. Xiancai, S. Wenxia, Physical Chemistry, 4th ed., China Higher Education Press, Beijing, 2004.

[13] R. Hino, K. Haga, H. Aita, K. Sekita, Nucl. Eng. Des. 233 (2004) 363–375.

[14] J.A. Dean, Lange's Handbook of Chemistry, 13th ed., McGraw Hill Book Company, New York, 1985.

[15] W. Zongxin, Z. Zuoyi, Advanced Nuclear System and High-Temperature Gas-Cooled Reactor, Tsinghua University Press, Beijing, 2004.